

## Electrohydrodynamic “drop-and-place” particle deployment

C.-H. Chen, D. A. Saville, and I. A. Aksay<sup>a)</sup>

*Department of Chemical Engineering, Princeton University, Princeton, New Jersey 08544*

(Received 29 October 2005; accepted 7 March 2006; published online 13 April 2006)

The “drop-and-place” paradigm aims at delivering and positioning liquid drops using a pulsed electrohydrodynamic jet. On-demand drops much smaller than the diameter of the delivery nozzle may also contain particles. We report proof-of-concept experiments on the delivery of single 2  $\mu\text{m}$  diameter particles using a 50  $\mu\text{m}$  nozzle and identify the control parameters for dosing and positioning accuracies. A positioning accuracy at the micrometer level is achieved by eliminating contact line pinning on a hydrophobic surface and minimizing impingement-induced motion. The dosing statistics follow the random Poisson distribution, indicating that single-particle accuracy can be achieved using a gating mechanism. © 2006 American Institute of Physics.

[DOI: 10.1063/1.2191733]

Contemporary techniques for particle deployment can be roughly classified as robotic, lithography directed, and field directed. Robotic manipulation is accomplished using micro-electromechanical system (MEMS) effectors for pick and place or scanning probes such as atomic force microscope tips;<sup>1</sup> this category offers direct manipulation at the nanoscale but has contact contamination and low throughput. Lithography-directed manipulation uses microfabricated patterns to guide particle deployment;<sup>2</sup> this category offers batch manipulation but spatial resolution is limited and the technique is somewhat inflexible due to fixed lithographic patterns. Field-directed manipulation relies on field gradients to trap and move objects (e.g., optical tweezers<sup>3</sup>); this category offers nonintrusive manipulation but the type of particle and operating environments are restricted.

Here, we report an alternative technique for particle deployment where particles are delivered in micron-scale liquid drops produced by an electrohydrodynamic (EHD) mechanism. We are particularly interested in single-particle manipulation, the achievement of which enables a drop-and-place paradigm for manufacturing micro- and nanostructures. Our EHD approach takes advantage of the large neck-down ratio of the EHD cone-jet configuration which enables the production of micron-scale drops from millimeter-scale nozzles.<sup>4</sup> Based on our exploratory work, EHD drop and place can circumvent many of the aforementioned drawbacks and achieve flexible, noncontact manipulation of a variety of materials at relatively high precision (submicron) and high speed (kilohertz). Nevertheless, several issues deserve attention and are discussed below.

A thin Teflon tube is used as the delivery nozzle for EHD drop generation (50  $\mu\text{m}$  ID, 360  $\mu\text{m}$  OD; Upchurch 1930) with a high voltage pulse applied between the nozzle (grounded through a stainless steel union) and a conductive silicon substrate (negatively electrified); details of the process are described elsewhere.<sup>4</sup> The silicon substrates used here are either coated with chromium (contact angle  $\theta \sim 30^\circ$ ), or with gold and treated with 1-hexadecanethiol (Sigma-Aldrich CAS No. 2917-26-2), a hydrophobic reagent ( $\theta \sim 100^\circ$ ).<sup>5</sup> Each external voltage pulse produces a drop; and for multiple drop production, the nozzle is mounted on a

custom-built motion system with a single-shaft stepping motor (MicroLynx-4; Intelligent Motion Systems, Marlborough, CT). Sulfate latex spheres (2.0  $\mu\text{m}$  diameter, Interfacial Dynamics 1-2000) are dispersed at a weight concentration of  $8.0 \times 10^{-5}$  (w/w) in de-ionized water with a conductivity of  $0.9 \times 10^{-4}$  S/m. In some experiments, red fluorescent dye (28 nm spheres, Duke Scientific R25) is added at  $1.0 \times 10^{-4}$  (w/w) to trace the deployed drops.

Figure 1 shows an array of drops produced by a pulsed EHD jet. The inset picture shows a sample cone-jet configuration emitting from an electrified liquid meniscus. A single external voltage pulse typically produces one drop, enabling on-demand drop generation. In another paper, we reported a scale analysis of pulsed EHD drop formation.<sup>4</sup> This analysis provides design guidelines for the drop volume and generation frequency. Despite the intrinsic pulsations resulting from the viscosity-limited flow rate, we showed that the drop formation process appears steady for a sufficiently long (compared to the cycle of intrinsic pulsation) external pulse.<sup>4</sup> The apparent steadiness is also supported by the array of fluores-

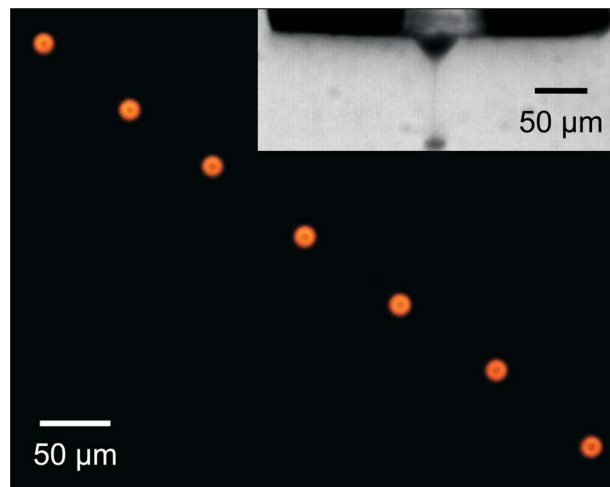


FIG. 1. (Color online) Drop formation by a pulsed EHD jet on a surface with a contact angle of  $\theta \sim 100^\circ$ . An external voltage pulse leads to cone-jet transition of the electrified liquid meniscus and produces a drop on the counter electrode (inset). The drop formation process is highly reproducible as indicated by an array of fluorescent spots as drop residue after solvent evaporation. Electrical configuration: voltage=1.2 kV, nozzle-to-collector separation=140  $\mu\text{m}$ , and pulse duration=7.5 ms.

<sup>a)</sup>Electronic mail: iaksay@princeton.edu

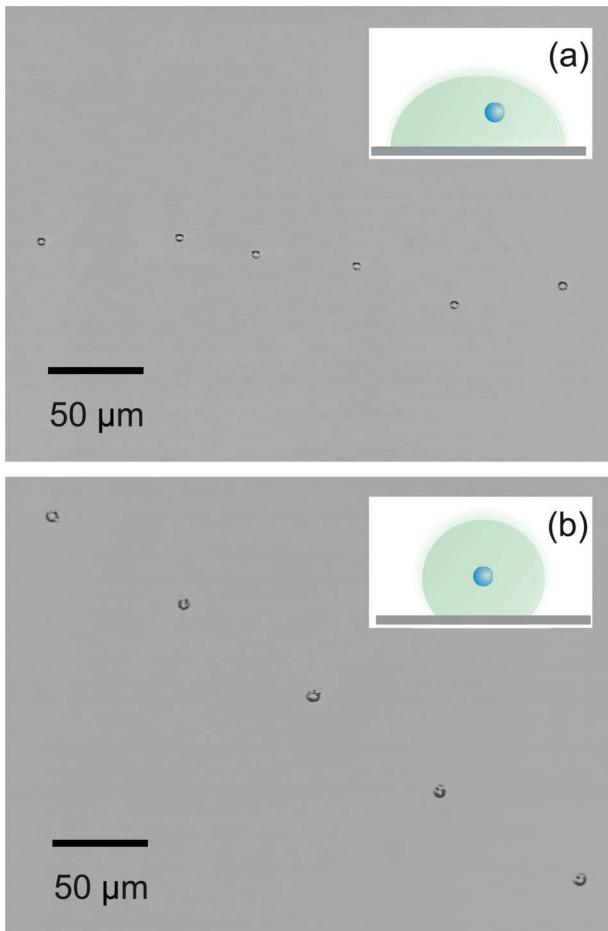


FIG. 2. (Color online) Improved positioning accuracy by tuning the surface wettability. The substrates used to collect  $2\ \mu\text{m}$  spheres are (a) chromium-coated silicon substrate ( $\theta \sim 30^\circ$ ); (b) Gold-coated substrate treated with 1-hexadecanethiol, a hydrophobic reagent ( $\theta \sim 100^\circ$ ). Fluorescent dye is added to (b) to show the contact area between the colloidal drops and the substrate. Electrical configuration is the same as Fig. 1.

cent spots (residues after solvent evaporation) showing the reproducibility of the drop formation process.

Guided by these insights, we utilized pulsed EHD drops as a transport medium for colloidal particles. There are two major challenges in implementing drop and place of single colloids: (i) positioning accuracy, the ability to place particles precisely at a predetermined location and (ii) dosing accuracy, the control over how many particles are in each droplet. The scaling laws<sup>4</sup> are important design guidelines: the accuracy of drop positioning is limited by the EHD jet diameter; the average number of particles dosed is related to drop volume and particle concentration. Here, we explore the possibility of delivering single particles at precise locations.

The positioning accuracy can be improved by tuning the surface wettability, as shown in Fig. 2. Here, an array of  $2\ \mu\text{m}$  spheres was deployed via 52 pL colloidal drops (statistically one  $2\ \mu\text{m}$  particle per drop), respectively, on hydrophilic ( $\theta \sim 30^\circ$ ) and hydrophobic ( $\theta \sim 100^\circ$ ) substrates. By using a more hydrophobic surface, the positioning accuracy is improved by an order of magnitude (to approximately  $2\ \mu\text{m}$ ). This positioning accuracy is comparable to the jet diameter of  $4 \pm 2\ \mu\text{m}$ . The order-of-magnitude improvement in positioning accuracy is achieved through the elimination of contact line pinning and minimization of impingement-induced drop motion. On a hydrophilic surface, contact line

pinning leads to the “coffee-stain” pattern in which colloids deposit at the edge of the drop upon solvent evaporation;<sup>6</sup> pinning effects are reduced or eliminated on a hydrophobic surface.<sup>7</sup> Since the contact area between the evaporating drop and hydrophobic surface is smaller, the drop residue on a hydrophobic surface is significantly smaller than a hydrophilic one. However, the outstanding positioning accuracy cannot be solely attributed to hydrophobicity. In fact, inkjet printing of polymer drops on a hydrophobic surface leads to “well-defined dots” (i.e., minimal drop residue) but poor positioning accuracy.<sup>8</sup>

In addition to low surface wettability, restricted drop motion on the substrate is essential to achieving good positioning accuracy. In this respect, relatively gradual drop formation by EHD jet accumulation is better than the abrupt drop detachment characteristic of inkjet printing because the former introduces far less momentum to the drop. The inertial force of jet impingement ( $F_m$ ) scales as

$$F_m \sim \frac{\Delta(mv)}{\Delta t} \sim \frac{\Delta m}{\Delta t} v_j \sim \pi \rho r_j^2 v_j^2, \quad (1)$$

where  $v_j$  is the jet velocity (assumed uniform and constant),  $\Delta m/\Delta t$  is the incoming mass flow rate,  $\rho$  is the liquid density, and  $r_j$  is the jet radius. The capillary force due to contact-angle hysteresis is<sup>9,10</sup>

$$F_c \sim \pi \gamma r_d (\cos \theta_r - \cos \theta_a), \quad (2)$$

where  $\gamma$  is the liquid surface tension,  $r_d$  is the radius of the contact circle between the drop and the surface, and  $\theta_r$  and  $\theta_a$  are the receding and advancing contact angles, respectively. To move a drop on a surface, the driving force needs to overcome the capillary force  $F_c$  due to the difference between advancing and receding angles.<sup>9,10</sup> Since the drops in our system are substantially smaller than the capillary length ( $\sqrt{\gamma/\rho g} \sim 3\ \text{mm}$  for water, where  $g$  is the gravitational acceleration), gravity alone cannot drive drop motion on a substrate. In the EHD drop formation process reported here,  $\rho \sim 1 \times 10^{-3}\ \text{kg/m}^3$ ,  $\gamma \sim 10^{-1}\ \text{N/m}$  (water);  $r_j \sim 1\ \mu\text{m}$ ,  $r_d \sim 10\ \mu\text{m}$  (measured);  $v_j \sim 1\ \text{m/s}$  (calculated from flow rate and jet radius);  $\theta_r \sim 90^\circ$ ,  $\theta_a \sim 110^\circ$ .<sup>5</sup> Hence,

$$\frac{F_m}{F_c} \sim \frac{\rho r_j^2 v_j^2}{\gamma r_d (\cos \theta_r - \cos \theta_a)} \sim 10^{-2}, \quad (3)$$

the inertial force, even if applied parallel to the substrate, is two orders of magnitude less than the capillary force arising from contact-angle hysteresis. Accordingly, capillary forces serve to restrict center-of-mass motion of drops on the substrate.

Two important guidelines for improving positioning accuracy can be derived by comparing inertial and capillary forces, as in Eq. (3). First, due to reduced impingement forces, gradual delivery is superior to abrupt drop formation. In the work of de Gans and Schubert,<sup>8</sup> inkjet drops of  $\sim 100\ \mu\text{m}$  arrive at the substrate at  $\sim 1\ \text{m/s}$  speed, giving rise to a substantially larger inertial force ( $F_m/F_c \sim 10$ ); hence a slight deviation ( $\sim 5^\circ$ ) from perpendicular arrival at the substrate can result in substantial center-of-mass drop motion. Second, there is an optimum contact angle for positioning accuracy. On a hydrophilic surface with a very low contact angle (e.g.,  $\theta \leq 30^\circ$ ), contact line pinning adversely affects positioning accuracy.<sup>6</sup> On a superhydrophobic surface with contact angle approaching  $180^\circ$  (e.g.,  $\theta \geq 150^\circ$ ), the

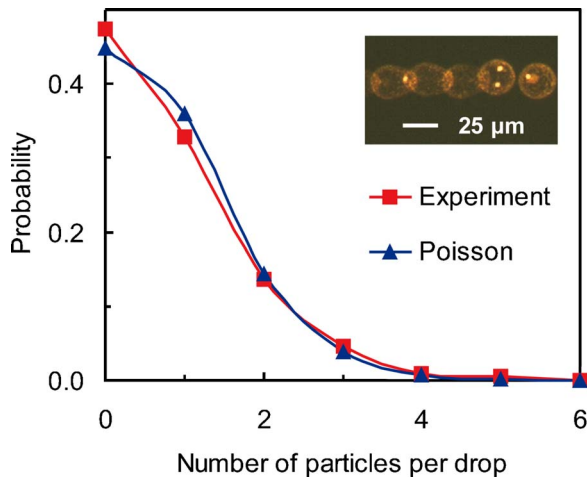


FIG. 3. (Color online) Poisson statistics of EHD drop and place. Equally sized drops are produced by a pulsed jet from a homogeneous aqueous suspension of  $2\ \mu\text{m}$  particles and fluorescent dye (inset). (■): the statistics for the number of particles per drop for 200 drops; (▲): Poisson distribution for a measured average of 0.80 particles per drop. Electrical configuration: voltage=1.6 kV, separation=90  $\mu\text{m}$ , and pulse duration=5.0 ms.

contact area becomes so small ( $r_d \rightarrow 0$ ) that a slight inertial force (or gravitational force) can overcome contact-angle hysteresis and leads to poor positioning accuracy.<sup>10</sup>

Although single-particle delivery can be achieved in consecutive drops as shown in Fig. 2(a), the particle dosing statistics for EHD drops are those of a random Poisson distribution (Fig. 3). Using a suspension of  $2\ \mu\text{m}$  spheres dispersed in de-ionized water, a total of 200 equally sized, 42 pl drops were produced and the number of particles carried per drop counted. Although the particle dispersion is homogeneous, particles arrive at the EHD nozzle in a random fashion. A representative set of results where the number of particles per drop is essentially identical to that from a Poisson distribution is shown in Fig. 3. Poisson statistics are also observed in cell sorting in which individual cells are detected and sorted in a mechanically generated droplet stream.<sup>11</sup> This similarity in dosing statistics indicates that the EHD process does not alter the random characteristics of particle appearance in a drop. Moreover, the similarity suggests that a gating mechanism could be used to achieve single-particle dosing accuracy. Such a system might employ fluorescence detection upstream of the EHD nozzle and electric deflection

downstream, similar to the scheme used in fluorescence-activated cell sorting.<sup>11</sup>

We have demonstrated the potential of single-particle deployment through colloidal drops and identified parameters controlling the dosing and positioning accuracies of EHD drop and place. Two features of the technique—the high voltage (kilovolts) required for the cone-jet transition and the relatively high jet speed ( $\sim 1\ \text{m/s}$ )—may be intrinsic limitations for some applications. Although we did not encounter problems with splashing, if encountered it can be avoided under vacuum.<sup>12</sup> EHD drop and place addresses some of the limitations of other methodologies noted earlier. Nevertheless, it is not a panacea and many features of the current configuration deserve attention. For example, micrometer-level poisoning accuracy was achieved on a hydrophobic, conducting substrate; achieving comparable accuracy on nonconducting substrates with a broader range of wettabilities is a challenge. Also, a gating mechanism may be required for consistent, single-particle deployment. Alternatively, EHD drop and place may be used as a method for assembly of organized clusters.<sup>13</sup>

This work was supported by Directed Technologies Inc., NASA Biologically Inspired Materials Institute (BIMat) under award No. NCC-1-02037, and ARO-MURI under award No. W911NF-04-1-0170. The authors thank P. Jiang, S. Korkut, W. D. Ristenpart, and H. C. Schniepp for helpful discussions.

<sup>1</sup>T. Fukuda, F. Arai, and L. X. Dong, Proc. IEEE **91**, 1803 (2003).

<sup>2</sup>J. Aizenberg, P. V. Braun, and P. Wiltzius, Phys. Rev. Lett. **84**, 2997 (2000).

<sup>3</sup>D. G. Grier, Nature (London) **424**, 810 (2003).

<sup>4</sup>C.-H. Chen, D. A. Saville, and I. A. Aksay, Appl. Phys. Lett. (submitted).

<sup>5</sup>H. A. Biebuyck and G. M. Whitesides, Langmuir **10**, 2790 (1994).

<sup>6</sup>R. D. Deegan, O. Bakajin, T. F. Dupont, G. Huber, S. R. Nagel, and T. A. Witten, Nature (London) **389**, 827 (1997).

<sup>7</sup>P. Takhistov and H. C. Chang, Ind. Eng. Chem. Res. **41**, 6256 (2002).

<sup>8</sup>B.-J. de Gans and U. S. Schubert, Langmuir **20**, 7789 (2004); see also [www.microdrop.de](http://www.microdrop.de), detailing the inkjet printer.

<sup>9</sup>E. B. Dussan, J. Fluid Mech. **137**, 1 (1983).

<sup>10</sup>D. Richard and D. Quere, Europhys. Lett. **48**, 286 (1999).

<sup>11</sup>J. V. Watson, *Introduction to Flow Cytometry* (Cambridge University Press, New York, 1991).

<sup>12</sup>L. Xu, W. W. Zhang, and S. R. Nagel, Phys. Rev. Lett. **94**, 184505 (2005).

<sup>13</sup>V. N. Manoharan, M. T. Elsesser, and D. J. Pine, Science **301**, 483 (2003).